Influence of negative ions on the plasma boundary sheath

R. Deutsch and E. Räuchle
Institut für Plasmaforschung, Universität Stuttgart, Pfaffenwaldring 31, 7000 Stuttgart 80, Germany
(Received 21 January 1992; revised manuscript received 18 June 1992)

The collisionless boundary sheath of a plasma containing additionally negative ions and secondary electrons is investigated theoretically. Bohm's criterion is generalized for such plasmas. The following effects are considered. (i) For negative-ion densities less than a critical value, the negative ions are captured by the positive ions through Coulomb collisions in the bulk plasma and in the presheath. As a consequence, the negative ions move together with the positive ions to the cathode. The critical density is determined by the collision frequencies of the negative ions with the positive ions and with the neutral atoms. (ii) Negative ions penetrating into the collisionless boundary sheath together with the positive ions are reflected by the electric field. As a consequence a double layer appears with a maximum of the electric field within the sheath. (iii) Secondary electrons emitted by the electrode reduce the field in the sheath and can form a virtual cathode. The theoretical results are in good agreement with experimental measurements.

PACS number(s): 52.40.Hf, 52.80.Hc

I. INTRODUCTION

The theoretical description and the understanding of processes in the boundary layer between the plasma and the solid surface is of importance for plasma processing, e.g., sputtering, etching, or thin-film deposition. Ions and electrons are accelerated in the electric field of the boundary sheath; the shape and the magnitude of the field determine the energy and flux of the particles at the surface and consequently the etching and the deposition rates. The structure of the boundary sheath was analyzed up to now for plasmas which contain only positive ions and electrons [1–4]. Plasmas containing also negative ions (e.g., halogens or oxygen) are of importance in plasma processing. The traditional theory of the current-voltage characteristics [1] was extended to plasmas with negative ions [5–8], however without any analysis of the field structure and particle motion in the sheath. In this paper the structure of the boundary sheath, the electric field, the particle motion, and the charge-density distribution in the sheath are investigated for plasmas which contain not only positive but also negative ions and secondary electrons. The experiments of Gottscho *et al.* [9–11] are suited to clarify the structure of the plasma boundary sheath. Using temporally and spatially resolved laser spectroscopy (optogalvanic signals and Stark-mixed laser-induced fluorescence spectra), Gottscho *et al.* [9–11] determined experimentally the electric-field distribution in the plasma boundary sheath in the neighborhood of the electrodes. The field structure in the collision-dominated regions in the vicinity of the anode and in the presheath of the cathode can be explained by the model of Boeuf based on macroscopic fluid equations with diffusion coefficients and drift velocities and the neglect of inertial effects [12].

The largest potential gradients in glow discharges exist in the cathode-fall region and the particles change their energy by a large amount in this region. Approaching the cathode, the electron and ion densities decrease and space charges are built up here. The plasma can be considered to be collisionless within the sheath [1–3]. The collisions which have the shortest mean free path in the sheath are those between ions and neutral atoms. The experiments of Gottscho *et al.* [9–11] were performed at a filling gas pressure of 0.1–0.3 Torr. In this case the mean free path for collisions of charged particles with the neutral background is of the order of the thickness of the cathode-fall region. Hence the collisional model used for the anode region [12] and for the presheath [11] cannot be extended to the cathode fall. The inertia of the particles becomes decisive within the sheath. For plasmas with positive ions, good agreement was obtained between the results of the collisionless theory [4] and the experimental results for the field in the plasma sheath at the cathode [10]. This agreement led to the motivation to elaborate the collisionless sheath theory also for the plasmas containing negative ions. The theory and a comparison with experiment are presented in this paper.

In the bulk plasma and in the presheath the negative ions gain momentum from the electric field and as a result of collisions with other particles. In Sec. II it is shown that if the negative-ion density is less than a critical value, the momentum of a negative ion gained by Coulomb collisions with positive ions is larger than the momentum obtained from the electric field. In this case the negative ions are captured by the positive-ion flow moving together through the presheath into a part of the collisionless sheath. The negative ions are then reflected by the electric field (Secs. III–V). Because of this reflection a double layer inside the sheath is formed. The existence of such double layers has been observed experimentally [9,10]. In Sec. VII the theoretical results are compared with the experimental values. A good agreement is obtained.

II. NEGATIVE-ION CAPTURE BY THE POSITIVE-ION FLOW IN THE BULK PLASMA AND IN THE PRESHEATH

A quasineutral unmagnetized plasma in contact with a plane electrode (Fig. 1) is considered. It is assumed that inside the sheath the particle density is low enough that collisions can be neglected. The processes in the bulk plasma and in the presheath, which determine the ion density and the particle flow from the presheath into the sheath, strongly depend on the collisions; therefore in the presheath and in the bulk plasma just these processes are considered. The production of negative ions is determined by the dissociation, the attachment of electrons to molecules or radicals, and the charge-exchange processes. The equilibrium between these processes determines the negative-ion concentration, however they have only a small influence on the mean momentum of the ions [13]. The changes in the mean momentum of the negative ions are dominated by the elastic collisions, therefore only these collisions are taken into account here for the calculation of the mean velocity of the negative ions. The negative-ion density n_{S-} at the boundary between the sheath and presheath is prescribed as boundary value. The electron temperature T_e is assumed to be constant and in the range of a few electron volts, and the ion temperature T_i in the range of about 0.026 eV in equilibrium with the neutral atoms. For simplicity only one species of positive and negative ions is considered here with charges $\pm q$ and the masses m_+ and m_-. Within the plasma and the presheath quasineutrality is assumed:

$$n_+ = n_e + n_- \ , \tag{2.1}$$

where n_e is the electron density and n_+, n_- are, respectively, the densities of the positive and negative ions (n_n = neutral-atom density).

In order to formulate the momentum equations we observe that the mean momentum of a negative ion ($m_- \bar{\mathbf{v}}_-$) changes mainly by (i) the action of the electric field on the ion ($-q\mathbf{E}$), (ii) the momentum transfer from the positive ions through Coulomb collisions [$\nu_{-+} m_- (\bar{\mathbf{v}}_+ - \bar{\mathbf{v}}_-)$], (iii) the momentum transfer from the electrons [$\nu_{-e} m_- (\bar{\mathbf{v}}_e - \bar{\mathbf{v}}_-)$], and (iv) the momentum transfer from the neutral atoms [$\nu_{-n} m_- (\bar{\mathbf{v}}_n - \bar{\mathbf{v}}_-)$]. Therefore the momentum equation for a negative ion in the bulk plasma and presheath is

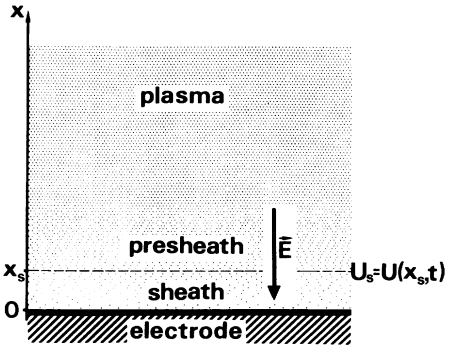

FIG. 1. Geometry of the plasma and plane electrode and notation.

$$\frac{d}{dt}(m_- \bar{\mathbf{v}}_-) = -q\mathbf{E} + \nu_{-+} m_- (\bar{\mathbf{v}}_+ - \bar{\mathbf{v}}_-) + \nu_{-e} m_- (\bar{\mathbf{v}}_e - \bar{\mathbf{v}}_-) + \nu_{-n} m_- (\bar{\mathbf{v}}_n - \bar{\mathbf{v}}_-) \ . \tag{2.2}$$

Similarly the equation of motion of the total system of ions is

$$\begin{aligned} \frac{d}{dt}(n_+ m_+ \bar{\mathbf{v}}_+ + n_- m_- \bar{\mathbf{v}}_-) &= (n_+ - n_-) q\mathbf{E} + \nu_{+e} n_+ m_+ (\bar{\mathbf{v}}_e - \bar{\mathbf{v}}_+) \\ &+ \nu_{-e} n_- m_- (\bar{\mathbf{v}}_e - \bar{\mathbf{v}}_-) + \nu_{+n} n_+ m_+ (\bar{\mathbf{v}}_n - \bar{\mathbf{v}}_+) \\ &+ \nu_{-n} n_- m_- (\bar{\mathbf{v}}_n - \bar{\mathbf{v}}_-) \ . \end{aligned} \tag{2.3}$$

Here $\bar{\mathbf{v}}_{+,-,e,n}$ is the mean velocity of positive ions, negative ions, electrons, and neutral atoms, respectively. The collision frequency for slowing down of negative ions by positive ions is ν_{-+}, for negative ions by electrons ν_{-e}, for negative ions by neutral atoms ν_{-n}, for positive ions by electrons ν_{+e}, and for positive ions by neutral atoms ν_{+n}. (The influence of the friction forces due to charge-exchange processes can be also included in $\nu_{\pm n}$.)

The electron mass is small whereas the neutral-atom mass and the masses of positive and negative ions are of the same order of magnitude. Therefore the momentum transfer between the positive and negative ions is much faster than the momentum transfer between electrons and ions. The collision frequencies ν_{-+} and ν_{-e} for Coulomb collisions can be approximated by Spitzer's formula [14],

$$\nu_{-+} = \begin{cases} 6.8\times10^{-8} n_+ \lambda_{-+} \dfrac{\sqrt{m_+ m_p}}{m_-} \left[1 + \dfrac{m_+}{m_-}\right] T_i^{-3/2} & \text{(for slow test ion)} \\ 9\times10^{-8} n_+ \lambda_{-+} \left[\dfrac{m_p}{m_-}\right]^{1/2} \left[1 + \dfrac{m_-}{m_+}\right] E_{\text{kin}}^{-3/2} & \text{(for fast test ion)} \end{cases} \tag{2.4a}$$

(2.4b)

and

$$\nu_{-e} = 1.6\times10^{-9} n_e \lambda_{-e} \frac{m_p}{m_-} T_e^{-3/2} \tag{2.5}$$

with m_p for the proton mass, E_{kin} for the test ion energy, and the corresponding Coulomb logarithms λ_{-+} and λ_{-e}. Densities are in units of cm^{-3}, energy and temperatures in units of eV. Taking into account that $kT_i < E_{\text{kin}} < kT_e$ for $T_e \gg T_i$ gives

$$\nu_{-+} \gg \nu_{-e} \ . \tag{2.6}$$

The mean-velocity differences in Eqs. (2.2) and (2.3) are of the same order of magnitude and reach values of the order of the ion acoustic velocity $\sqrt{kT_e/m_+}$ in the presheath, as will be discussed in Sec. IV. Therefore with Eq. (2.6) all terms connected with collisions between ions and electrons can be neglected in Eqs. (2.2) and (2.3). Since the mean velocity of the neutral atoms $\bar{v}_n \approx 0$ is also negligible and $\nu_{+n} \approx \nu_{-n} = \nu_n$, from (2.2) and (2.3) the closed system

$$\frac{d\bar{v}_-}{dt} + (\nu_{-+} + \nu_n)\bar{v}_- - \nu_{-+}\bar{v}_+ = -\frac{q}{m_-}E \ , \tag{2.7}$$

$$\frac{d\bar{v}_+}{dt} + (\nu_{+-} + \nu_n)\bar{v}_+ - \nu_{+-}\bar{v}_- = \frac{q}{m_+}E \tag{2.8}$$

is obtained with

$$\nu_{+-} = \frac{n_- m_-}{n_+ m_+}\nu_{-+} \ . \tag{2.9}$$

In a first approximation $\nu_{-+}, \nu_{+-}, \nu_n$ are taken as velocity-independent constant coefficients. For a given constant electric field E the solution of this system of differential equations (2.7) and (2.8) is

$$\bar{v}_- = A\exp(-\nu_n t) + B\nu_{-+}\exp[-(\nu_n + \nu_{+-} + \nu_{-+})t] + w_- \ , \tag{2.10}$$

$$\bar{v}_+ = A\exp(-\nu_n t) - B\nu_{+-}\exp[-(\nu_n + \nu_{+-} + \nu_{-+})t] + w_+ \ , \tag{2.11}$$

A and B are integration constants, and

$$w_- = \frac{m_-\nu_{-+} - m_+(\nu_{+-} + \nu_n)}{m_- m_+ \nu_n(\nu_{+-} + \nu_{-+} + \nu_n)}qE \ , \tag{2.12}$$

$$w_+ = \frac{m_-(\nu_{-+} + \nu_n) - m_+\nu_{+-}}{m_- m_+ \nu_n(\nu_{+-} + \nu_{-+} + \nu_n)}qE \ . \tag{2.13}$$

w_- and w_+ are the limiting velocities for $t \to \infty$,

$$\lim_{t\to\infty}\bar{v}_- \to w_- \ , \quad \lim_{t\to\infty}\bar{v}_+ \to w_+ \ . \tag{2.14}$$

With Eq. (2.9) there results

$$\frac{w_-}{w_+} = \frac{1 - \dfrac{n_-}{n_+} - \dfrac{m_+}{m_-}\dfrac{\nu_n}{\nu_{-+}}}{1 - \dfrac{n_-}{n_+} + \dfrac{\nu_n}{\nu_{-+}}} \ . \tag{2.15}$$

In the quasineutral case [Eq. (2.1)] with $n_+ > n_-$ the denominator of (2.15) is positive. The numerator changes its sign at the critical negative-ion density

$$n_-^* = \left(1 - \frac{\nu_n m_+}{\nu_{-+} m_-}\right)n_+ \ .$$

Therefore if the density of the negative ions is smaller than this critical density, $n_- < n_-^*$ the momentum transfer from the positive ions to the negative ions by Coulomb collisions is larger than the momentum change due to the electrostatic force $-qE$ and the retarding force of the collisions with neutral atoms. In this case the negative ions move in the same direction as the positive ions to the negatively charged electrode. The existence of this effect also results from Eq. (33) in Ref. [13].

$$n_- < n_-^* \tag{2.16}$$

is the condition for the capture of the negative ions by the positive-ion flow which is accelerated in the electric field of the plasma. Therefore if in the plasma $n_- < n_-^*$, not only the positive ions, but also the negative ions move together from the positively charged bulk plasma through the presheath into the sheath in the direction of the negative electrode. If $n_- > n_-^*$ the positive ions and the negative ions move in opposite directions driven by the dominant electrostatic forces and the collisions have only retarding effects. In this paper low negative-ion densities are assumed $n_- < n_-^*$. The velocities $\bar{v}_+$ and $\bar{v}_-$ at the boundary of the presheath and sheath are considered to be parallel and of the same order of magnitude.

III. THE MODEL OF THE COLLISIONLESS SHEATH

A. Distribution functions at $x = x_S$

At the interface between the sheath and presheath (at $x = x_S$ in Fig. 1) the positive ions are moving from the presheath into the sheath with average velocity $v_{S+} < 0$ and the negative ions with $v_{S-} < 0$. It is assumed that the collisions in the sheath can be neglected and that all ions which reach the electrode are absorbed. At $x = x_S$ the velocity distributions are approximated by shifted Maxwellian distributions. The velocity spread around the mean velocity is characterized by the ion temperature T_i.

1. Positive ions

The velocity distribution at $x = x_S$ is described by

$$f_+(v_S) = f_{+0}\exp\left[-\frac{m_+(v_S - v_{S+})^2}{2kT_i}\right] \ . \tag{3.1}$$

The density n_{S+} of the positive ions which penetrate into the sheath at $x = x_S$ is

$$n_{S+} = \int_{-\infty}^{0} f_+(v_S)dv_S \ . \tag{3.2}$$

The mean ion velocity in plasmas with only positive ions must satisfy the Bohm criterion [2,3] $v_{S+}^2 \geq kT_e/m_+$. It is supposed here that a similar criterion should exist also for plasmas containing negative ions. The analytical expression of the Bohm criterion extended to plasmas with negative ions will be formulated in Eq. (4.5). From the Bohm criterion results, that the maximum of $f_+(v_S)$ in (3.1) is shifted to velocities of the order of $v_S \leq -\sqrt{kT_e/m_+}$ and for $T_e \gg T_i$ it is a narrow function. Therefore the upper integration limit can be taken approximately as $v_S = \infty$. From (3.1) and (3.2), $f_{+0} = n_{S+}\sqrt{m_+/2\pi kT_i}$ and the distribution function

(3.1) is

$$f_+(v_S)=n_{S+}\sqrt{m_+/2\pi kT_i}\exp\left[-\frac{m_+(v_S-v_{S+})^2}{2kT_i}\right]. \tag{3.1'}$$

2. Negative ions

In order to obtain the distribution function for the negative ions it must be taken into account that the negative ions, which enter the sheath with a velocity smaller than a critical value v_S^*, are reflected by the electric field of the negatively biased electrode. If $(|v_{S-}|-v_S^*)^2$ is sufficiently large that

$$\exp\left[-\frac{m_-(|v_{S-}|-v_S^*)^2}{2kT_i}\right]\ll 1\ , \tag{3.3}$$

the distribution function can be easily normalized. Since $|v_{S-}|$ is of the order of $|v_{S+}|$ and $|U_S-U(0,t)|$ is of the order kT_e/q, condition (3.3) is satisfied in the greatest part of the period during the voltage oscillations of rf discharges when $T_e \gg T_i$. This case is considered in this paper.

If condition (3.3) is satisfied for $T_e \gg T_i$ two different distributions of the negative-ion velocities v_S at $x=x_S$ exist (see Fig. 2).

(i) If $|v_{S-}|<v_S^*$ most of the negative ions are reflected. Only a negligible number of negative ions in the tail of the Maxwell distribution reach the electrode and in this case the distribution functions result [see Fig. 2(a)]:

For the incident particles $(0>v_S>-v_S^*)$,

$$f_-^{(i)}(v_S)=\tfrac{1}{2}n_{S-}\sqrt{m_-/2\pi kT_i}\exp\left[-\frac{m_-(v_S-v_{S-})^2}{2kT_i}\right]; \tag{3.4a}$$

for the reflected particles $(0<v_S<v_S^*)$,

$$f_-^{(r)}(v_S)=\tfrac{1}{2}n_{S-}\sqrt{m_-/2\pi kT_i}\exp\left[-\frac{m_-(v_S+v_{S-})^2}{2kT_i}\right]; \tag{3.4b}$$

and for the particles which traverse the sheath $(v_S<-v_S^*)$,

$$f_-^{(t)}(v_S)\approx 0\ . \tag{3.4c}$$

(ii) If $v_{S-}<-v_S^*$ most of the negative ions traverse the sheath and only a few particles in the tail of the Maxwell distribution are reflected. Therefore the distribution functions of the negative ions are [see Fig. 2(b)]

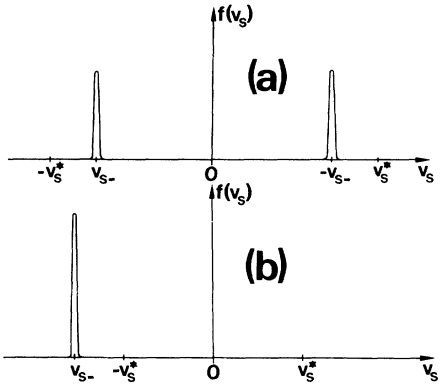

FIG. 2. Velocity distribution of the negative ions at $x=x_S$ for (a) $|v_{S-}|<v_S^*$ and (b) $v_{S-}<-v_S^*$.

$$f_-^{(i)}(v_S)\approx f_-^{(r)}(v_S)\approx 0 \quad \text{for } |v_S|<v_S^* \tag{3.5a}$$

and

$$f_-^{(t)}(v_S)=n_{S-}\sqrt{m_-/2\pi kT_i}\exp\left[-\frac{m_-(v_S-v_{S-})^2}{2kT_i}\right] \quad \text{for } |v_S|>v_S^*\ . \tag{3.5b}$$

The functions in (3.4) and (3.5) are normalized to the density n_{S-} of the negative ions at $x=x_S$ as in Eq. (3.1').

B. Distribution functions and densities in the boundary sheath

In order to extend the distribution functions for $x=x_S$ into the interior of the collisionless sheath $0<x<x_S$, energy conservation yields

$$\tfrac{1}{2}m_+v^2+qU(x)=\tfrac{1}{2}m_+v_S^2+qU_S \tag{3.6}$$

for the positive ions and

$$\tfrac{1}{2}m_-v^2-qU(x)=\tfrac{1}{2}m_-v_S^2-qU_S \tag{3.7}$$

for the negative ions. Substituting v_S from Eqs. (3.6) and (3.7) in (3.1'), (3.4a), (3.4b), and (3.5b), introducing $\alpha=n_{S-}/n_{Se}$ for the ratio of the negative-ion density to the electron density at $x=x_S$, and using the quasineutrality condition $n_{S-}+n_{Se}=n_{S+}=n_S$, then because of the symmetry of (3.4a) and (3.4b) with respect to the substitution $v_S\to -v_S$ the distribution functions of the ions inside the sheath are found to be

$$f_+(x,v)=n_S\sqrt{m_+/2\pi kT_i}\exp\left[-\frac{m_+\left[\left[v^2+\frac{2q}{m_+}[U(x)-U_S]\right]^{1/2}+v_{S+}\right]^2}{2kT_i}\right] \tag{3.8}$$

for the positive ions for $v<0$ and

$$f_-(x,|v|)=\frac{\alpha n_S}{1+\alpha}\sqrt{m_-/2\pi kT_i}\exp\left[-\frac{m_-\left[\left[v^2-\frac{2q}{m_-}[U(x)-U_S]\right]^{1/2}+v_{S-}\right]^2}{2kT_i}\right] \tag{3.9}$$

for the negative ions with $f_-(x,|v|)=f_-(x,v)+f_-(x,-v)$.

The ion density within the sheath can be obtained by integrating the distribution functions (3.8) and (3.9):

$$n_+(x)=\left[\frac{m_+}{2\pi kT_i}\right]^{1/2} n_S \int_{v_{S+}}^{\infty} \frac{(z-v_{S+})\exp\left[-\frac{m_+ z^2}{2kT_i}\right]dz}{\left[(z-v_{S+})^2-\frac{2q}{m_+}[U(x)-U_S]\right]^{1/2}} \tag{3.10}$$

for the positive-ion density and

$$n_-(x)=\left[\frac{m_-}{2\pi kT_i}\right]^{1/2} \frac{\alpha n_S}{1+\alpha} \int_{z^*}^{\infty} \frac{(z-v_{S-})\exp\left[-\frac{m_- z^2}{2kT_i}\right]dz}{\left[(z-v_{S-})^2+\frac{2q}{m_-}[U(x)-U_S]\right]^{1/2}} \tag{3.11}$$

for the negative-ion density.

In (3.10) and (3.11) the substitutions $z=\sqrt{v^2\pm(2q/m_\pm)[U(x)-U_S]}+v_{S\pm}$ and $z^*=v_{S-}+\sqrt{(2q/m_-)[U_S-U(x)]}$ are used.

The electrons are described by the Boltzmann distribution

$$n_e(x)=\frac{n_S}{1+\alpha}\exp\left[\frac{q[U(x)-U_S]}{kT_e}\right]. \tag{3.12}$$

C. Electric field in the boundary sheath

From Poisson's equation

$$\Delta U=\frac{q}{\epsilon_0}[n_e(x)+n_-(x)-n_+(x)] \tag{3.13}$$

together with Eqs. (3.10)–(3.12) the following differential equation for the electric potential inside the sheath is obtained:

$$\frac{d^2U}{dx^2}=\frac{n_S q}{\epsilon_0}\left\{\frac{1}{1+\alpha}\exp\left[\frac{q[U(x)-U_S]}{kT_e}\right]+\frac{\alpha}{1+\alpha}\left[\frac{m_-}{2\pi kT_i}\right]^{1/2}\int_{z^*}^{\infty}\frac{(z-v_{S-})\exp\left[-\frac{m_- z^2}{2kT_i}\right]dz}{\left[(z-v_{S-})^2+\frac{2q}{m_-}[U(x)-U_s]\right]^{1/2}}\right.$$
$$\left.-\left[\frac{m_+}{2\pi kT_i}\right]^{1/2}\int_{v_{S+}}^{\infty}\frac{(z-v_{S+})\exp\left[-\frac{m_+ z^2}{2kT_i}\right]dz}{\left[(z-v_{S+})^2-\frac{2q}{m_+}[U(x)-U_S]\right]^{1/2}}\right\}. \tag{3.14}$$

In plasmas with negative ions there is a deviation from quasineutrality at the interface between the presheath and sheath in contrast to the plasmas without negative ions (see Sec. VII). For simplicity it is assumed here as a first approximation that the deviation from quasineutrality is small and that the boundary conditions at $x=x_S$ are given as usual [3,4] by $dU/dx\approx 0$ and $U(x_S)=U_S$. A first integration of Eq. (3.14) at $T_e\gg T_i$ leads to

$$\frac{d\varphi}{d\xi}=-\sqrt{8f(\varphi)} \tag{3.15}$$

with

$$f(\varphi)=\frac{1}{1+\alpha}\left[\exp\left[\frac{\beta_+-\varphi}{2}\right]-1\right]$$
$$+\frac{\alpha\beta_+\kappa}{1+\alpha}\left[\frac{\Theta\beta_+\kappa}{2\pi}\right]^{1/2}\int_{\eta^*}^{\infty}\left\{\left[(\eta+1)^2+\frac{1}{\kappa}\left[1-\frac{\varphi}{\beta_+}\right]\right]^{1/2}-\eta-1\right\}(\eta+1)\exp\left[-\frac{\Theta\kappa\beta_+}{2}\eta^2\right]d\eta$$
$$+\beta_+\left[\frac{\Theta\beta_+}{2\pi}\right]^{1/2}\int_{-1}^{\infty}\left\{\left[(\eta+1)^2-1+\frac{\varphi}{\beta_+}\right]^{1/2}-\eta-1\right\}(\eta+1)\exp\left[\frac{-\Theta\beta_+}{2}\eta^2\right]d\eta. \tag{3.16}$$

Here the following notations are used:

$$\varphi=\frac{m_+v_{S+}^2-2q(U-U_S)}{kT_e}\ ,\quad \beta_\pm=\frac{m_\pm v_{S\pm}^2}{kT_e}\ ,\quad \kappa=\frac{m_-v_{S-}^2}{m_+v_{S+}^2}\ ,$$
$$\eta=-\frac{z}{v_{S\pm}}\ ,\quad \eta^*=-\frac{z^*}{v_{S-}}\ ,\quad \xi=\frac{x}{\lambda_D}\ ,\quad \Theta=\frac{T_e}{T_i}\ ,\quad \lambda_D=\left[\frac{\epsilon_0 kT_e}{q^2n_S}\right]^{1/2}\ . \tag{3.17}$$

IV. GENERALIZED BOHM CRITERION

In the extension [5–8] of Bohm's criterion to plasmas with negative ions, the capture of negative ions by positive ions through Coulomb collisions is not taken into account. Usually the Boltzmann distribution function is used for the negative ions in the same way as for the electrons. In this work Bohm's criterion is generalized to the case where not only a positive-ion flow but also a negative-ion flow traverses the boundary between the sheath and the presheath. It is assumed that the flow velocity exceeds the ion thermal velocity,

$$\beta_- \gg \frac{1}{\Theta}\ . \tag{4.1}$$

This is contrary to the case ($\beta_-=0$) treated in [5–8].

In order to obtain in (3.15) a real solution for the electric potential, the function $f(\varphi)$ must be positive. In the vicinity of $x=x_S$ the function $f(\varphi)$ is approximated by a series expansion in $\delta=\varphi-\beta_+$,

$$f(\varphi)=\frac{1}{8}\left\{\frac{1}{1+\alpha}-\frac{\alpha}{\beta_+\kappa\sqrt{\pi}(1+\alpha)}\int_{-1}^{\infty}\frac{1}{(\eta+1)^2}\exp\left[-\frac{\beta_+\kappa\Theta}{2}\eta^2\right]d\left[\left[\frac{\beta_+\kappa\Theta}{2}\right]^{1/2}\eta\right]\right.$$
$$\left.-\frac{1}{\beta_+\sqrt{\pi}}\int_{-1}^{\infty}\frac{1}{(\eta+1)^2}\exp\left[-\frac{\beta_+\Theta}{2}\eta^2\right]d\left[\left[\frac{\beta_+\Theta}{2}\right]^{1/2}\eta\right]\right\}\delta^2+\cdots>0\ . \tag{4.2}$$

For $\Theta\gg1$ only the contributions from $|\eta|\ll1$ are of importance in the integrals. Therefore, the integrands can be approximated by a series in η. After integration there results

$$\left\{\frac{1}{1+\alpha}-\frac{\alpha}{1+\alpha}\frac{1}{\beta_-}-\frac{1}{\beta_+}-\frac{3}{\Theta}\left[\frac{\alpha}{1+\alpha}\frac{1}{\beta_-^2}+\frac{1}{\beta_+^2}\right]\right\}\delta^2+\cdots>0\ . \tag{4.3}$$

For $\delta\to0$ and $\Theta\gg1$ there results from (4.3) the condition

$$\frac{1+\alpha}{\beta_+-3/\Theta}<1-\frac{\alpha}{\beta_--3/\Theta}\ . \tag{4.4}$$

The parameter values, which satisfy Eq. (4.4), lie outside of the hatched region of the β_+-β_- plane of Fig. 3. At $x=x_S$ the positive ions have a larger velocity than in plasmas without a captured negative-ion flow. In the case of $T_i=0$ there result two conditions from Eq. (4.4) for the velocities v_{S+} and v_{S-}. The left-hand side of Eq. (4.4) is positive. Therefore $1-\alpha/\beta_->0$ and there results

$$v_{S-}^2>\alpha kT_e/m_-=v_{B-}^2 \tag{4.5a}$$

for the negative-ion velocity v_{S-}. Using the definition (3.17) of β_+ and β_- Eq. (4.4) can be written in the form

$$v_{S+}^2>\left[\frac{1+\alpha}{1-\alpha kT_e/m_-v_{S-}^2}\right]kT_e/m_+=v_{B+}^2\ . \tag{4.5b}$$

The inequalities (4.5a) and (4.5b) correspond to the Bohm criterion if the condition (4.1) is satisfied. In the limit $\alpha\to0$ the criterion (4.5b) coincides with the usual Bohm criterion of plasmas with positive ions only.

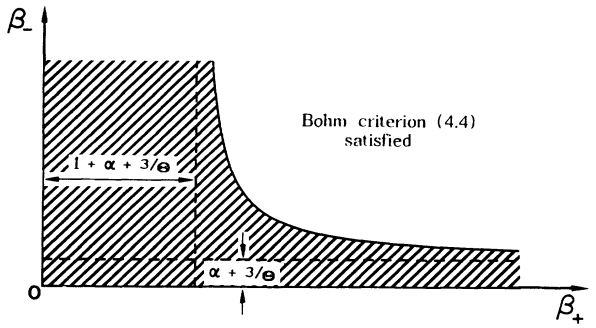

FIG. 3. Bohm limit in the $\beta_+-\beta_-$ plane.

V. REFLECTION OF THE NEGATIVE IONS

Because of the small mass of the electrons the plasma potential is usually positive with respect to the electrodes. In the collisionless sheath the positive ions are accelerated to the electrodes. The negative ions are slowed down and are eventually reflected by the electric field. This reflection is discussed in Sec. V A for $T_i=0$ and in Sec. V B for finite ion temperature.

A. Reflection of a cold negative-ion flow for $T_i=0$

1. *Criteria for ion reflection for $T_i=0$*

If the thermal motion of the ions can be neglected in comparison to that of the electrons, all negative ions enter with the same velocity v_{S-} and are slowed down within the sheath [see Eq. (3.7)]. If

$$U(0)-U_S<-\frac{m_-}{2q}v_{S-}^2$$

the negative ions are reflected totally (Fig. 4). At the point of reflection $x=x_r$

$$U(x_r)=U_S-\frac{m_-}{2q}v_{S-}^2 \ . \tag{5.1}$$

For cold ions ($T_i\to 0$) the integrals in (3.16) can be calculated analytically and the differential equation for the electric potential is found to be

$$\frac{d\varphi}{d\xi}=-\sqrt{8}\left\{\frac{1}{1+\alpha}\left[\exp\left[\frac{\beta_+-\varphi}{2}\right]-1\right]+\frac{\alpha\beta_+\kappa}{1+\alpha}\left\{\left[1+\frac{1}{\kappa}\left[1-\frac{\varphi}{\beta_+}\right]\right]^{1/2}-1\right\}+\beta_+\left[\left[\frac{\varphi}{\beta_+}\right]^{1/2}-1\right]\right\}^{1/2} . \tag{5.2}$$

The negative ions are reflected if the square root $\sqrt{1+(1-\varphi/\beta_+)/\kappa}$ on the right-hand side of Eq. (5.2) vanishes; this means if $\varphi=(1+\kappa)\beta_+$. For this value of φ the right-hand side of Eq. (5.2) is real only if

$$\alpha\le\alpha^*=\frac{1}{\sqrt{1+\kappa}}\left[1-\frac{1-\exp(-\beta_+\kappa/2)}{\beta_+(\sqrt{1+\kappa}-1)}\right] . \tag{5.3}$$

Equation (5.3) is the condition for the negative ions to be reflected.

In addition α is limited by the condition (2.16). Assuming to a first approximation that n_-/n_+ is constant in the presheath, condition (2.16) for the negative-ion capture can be formulated as an upper limit for α:

$$\alpha<\frac{\nu_{-+}m_- -\nu_n m_+}{\nu_n m_+} . \tag{5.4}$$

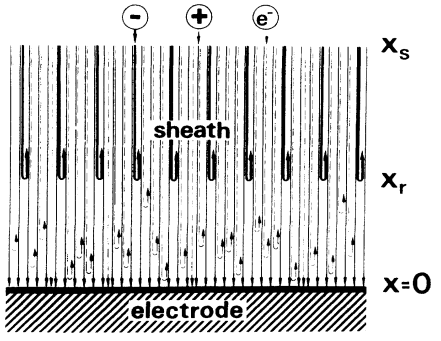

FIG. 4. Reflection of the negative ions in the sheath.

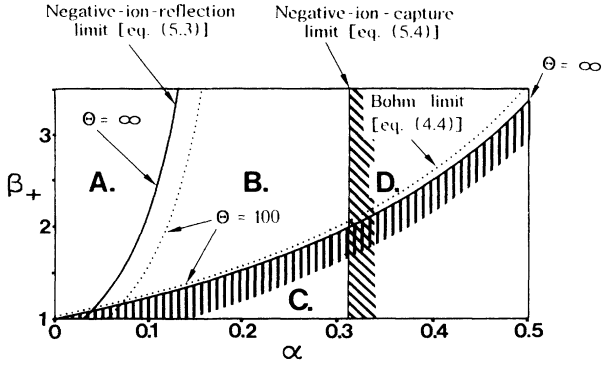

FIG. 5. α-β_+ parameter plane for $\beta_-=0.9$.

In Fig. 5 the reflection limit $\alpha=\alpha^*(\beta_+,\kappa)$ corresponding to Eq. (5.3), Bohm's criterion (4.5b), and condition (5.4) are plotted in the α-β_+ plane for $\beta_-=0.9$. The solid lines refer to $T_i=0$ and the dotted lines to $\Theta=T_e/T_i=100$. The α-β_+ plane is separated by these limiting lines into four regions: (i) In region D the criterion (5.4) for the capture of negative ions is not satisfied. (ii) In region C Bohm's criterion is not satisfied, therefore a stationary sheath does not exist in this parameter range. (iii) In regions A and B the Bohm criterion and condition (5.4) are satisfied. (iv) In region A the inequality (5.3) is valid and the negative ions are reflected. (v) In region B the inequality (5.3) is not satisfied; therefore the negative ions are slowed down and they fly to the electrode.

2. *Numerical results*

The numerical solution of Eq. (5.2) with the boundary condition $\varphi(x=0)=\varphi_0$ differs in regions A and B.

a. Region A. The calculated electric field E, normalized by $E^*=-kT_e/2q\lambda_D$, the normalized electric potential φ, the velocities of the positive and negative ions, normalized by the velocities at $x=x_S$, and the electric charge density ρ, normalized by qn_S inside the sheath as functions of the distance ξ from the electrode, are plotted in Fig. 6(a) for region A. The positive ions are accelerated to the electrode and the negative ions are slowed down and then reflected at $\xi=\xi_r$. The normalized potential increases monotonically in approaching the electrode. The electric field has a maximum at $\xi>\xi_r$ and a minimum at the point of reflection $\xi=\xi_r$. In the neighborhood of $\xi=\xi_r$ the velocity of the negative ions becomes small and therefore the density of these ions becomes larger than the positive-ion density and a double layer is formed. An increase of the relative negative-ion density α leads to an increase of the number of the reflected negative ions and of the changes in the field with more pronounced maxima and minima. For $\alpha=\alpha^*$ [see Eq. (5.3)] in the reflection point the field vanishes: $\mathbf{E}(\xi_r)=0$. This situation is plotted in Fig. 6(b).

b. Region B. In region B of Fig. 5 with $\alpha>\alpha^*$, the density of the negative ions during slowing down is large enough to produce a negative-ion concentration for a change in the sign of the electric field. In this case after reaching a minimum velocity, the negative ions will be

accelerated again to the electrode with no reflection.

The potential φ, electric field E, negative-, and positive-ion velocity $v_{\mp}$, and charge density ρ are plotted in Figs. 7(a)–7(e) as functions of ξ for typical parameter values $\alpha=0.3$, $\beta_+=2$, $\kappa=0.5$, and $\Theta=\infty$. It is shown that the positive ions are accelerated to the electrode up to the point $\xi_{\rm inv}$, where $\mathbf{E}(\xi_{\rm inv})=\mathbf{0}$, and then they are slowed down on their way to the electrode [Fig. 7(b)]. In contrast, the negative ions are slowed down up to $\xi=\xi_{\rm inv}$ and then they are accelerated [Fig. 7(c)]. In the neighborhood of $\xi=\xi_{\rm inv}$ a double layer develops inside the sheath [Fig. 7(d)]. The normalized voltage φ has a maximum at $\xi=\xi_{\rm inv}$ [Fig. 7(e)] and its value is limited to the interval

$$\beta_+ \le \varphi \le \varphi_{\max} . \tag{5.5}$$

Also $\varphi_{\max}$ must be less than $(1+\kappa)\beta_+$ to get a real value for the electric field from Eq. (5.2). The voltage between plasma and electrode is limited at the cathode by the large number of the negative ions which decrease the negative floating potential. As the voltage between cathode and anode changes the voltage between cathode and plasma remains in the interval given by (5.5); the maximum will be shifted in the sheath to the corresponding distance $\xi_{\rm inv}$. The normalized potential $\varphi_{\max}$ can be determined from $d\varphi/d\xi=0$ using Eq. (5.2), so that

$$1-\exp\left[\frac{\beta_+-\varphi_{\max}}{2}\right] -\alpha\kappa\beta_+\left\{\left[1+\frac{1}{\kappa}\left[1-\frac{\varphi_{\max}}{\beta_+}\right]\right]^{1/2}-1\right\} -(1+\alpha)\beta_+\left[\left[\frac{\varphi_{\max}}{\beta_+}\right]^{1/2}-1\right]=0 .$$

B. Reflection of negative ions for finite T_i

To characterize the structure of the collisionless sheath for finite T_i it is useful to consider again the α-β_+ plane of Fig. 5. The separation lines between regions A and B and regions B and C are shifted for finite $\Theta\gg1$ in comparison to the lines for $\Theta=\infty$ by a small amount. This is shown in Fig. 5 for finite T_i ($\Theta=100$) by the dotted lines.

To obtain the electric potential as a function of ξ, Eq. (3.15) is integrated numerically with the boundary condition $\varphi(x=0)=\varphi_0$.

1. Region A

In Fig. 8 two typical results for region A are plotted. The dependence of the normalized potential, electric field, and electric charge density on ξ are shown for the parameter values $\Theta=100$, $\beta_+=1.5$, and $\kappa=1$. Figure 8(a) shows results for $\alpha=0.1$; the normalized electric field

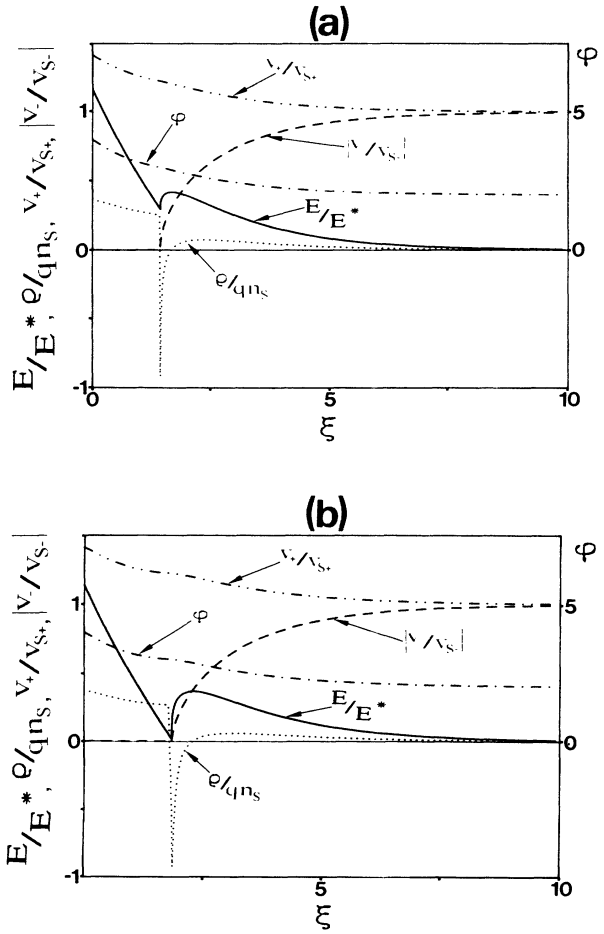

FIG. 6. (a) Sheath structure in region A for $\alpha=0.08$, $\beta_+=2$, $\kappa=0.5$, and $\Theta=\infty$. (b) Sheath structure for $\alpha=\alpha^*=0.1017$, $\beta_+=2$, $\kappa=0.5$, and $\Theta=\infty$.

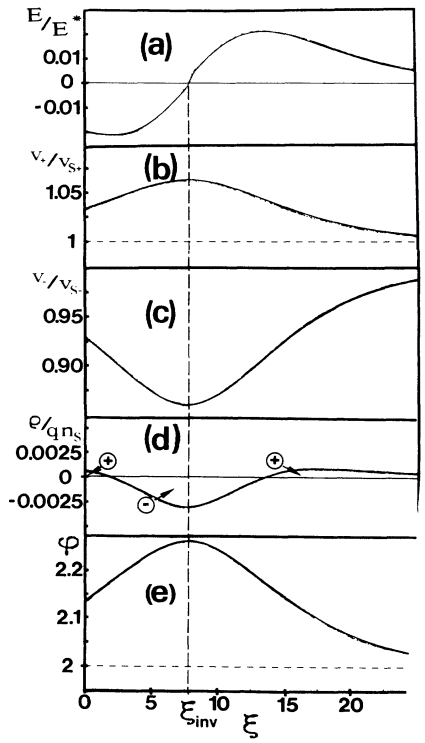

FIG. 7. Sheath structure in region B for $\alpha=0.3$, $\beta_+=2$, $\kappa=0.5$, and $\Theta=\infty$.

changes monotonically with ξ and the charge density in the sheath is everywhere positive. Figure 8(b) shows results for $\alpha=0.145$. Here a double layer exists inside the sheath with a maximum and a minimum of the electric field. This is a result of reflection of the negative ions. The thermal motion of the ions leads to a smoothing of the maximum and of the minimum of the $E(\xi)$ curve (compare Fig. 6 with Fig. 8). The reflected negative ions cause a disturbance in the field, compared to the case with no negative ions. This disturbance increases with an increase of the relative number α of the negative ions. For $\alpha=0.1$ [Fig. 8(a)] only a deformation in the $E(\xi)$ curve occurs but no double layer develops; as α increases the deformation increases, a maximum and a minimum in $E(\xi)$ occur, and a sheath with negative charge density appears. At the border between regions A and B, indicated in Fig. 5 by the dotted line, $E_{\min}$ cancels.

2. Region B

The influence of the ion temperature on the solution of Eq. (3.15) is negligible for $\Theta \gg 1$. Therefore the results obtained from Eq. (5.2) for $T_i=0$ can be applied also for $T_i \ll T_e$.

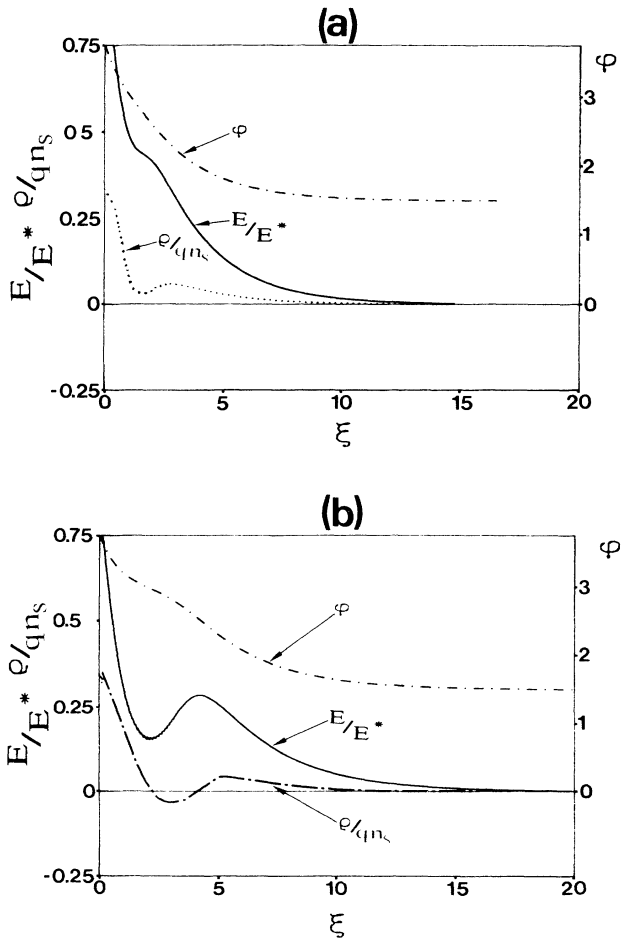

FIG. 8. (a) Sheath structure in region A for $\Theta=100$, $\alpha=0.1$, $\beta_+=1.5$, and $\kappa=1$. (b) Sheath structure in region A for $\Theta=100$, $\alpha=0.145$, $\beta_+=1.5$, and $\kappa=1$.

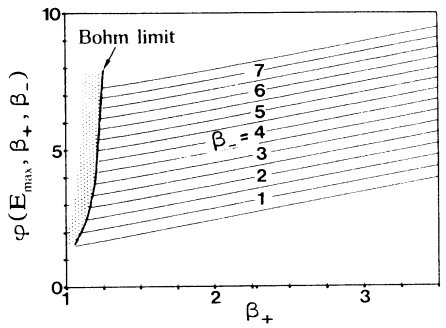

FIG. 9. $\varphi(E_{\max})$ as a function of β_+ and β_- for $\alpha=\alpha^*$ and $\Theta=\infty$.

C. Maximum and minimum of the electric field

The negative ions moving with the mean velocity v_{S-} at $x=x_S$ are reflected at $x=x_r$, where $U(x_r)=U_S-m_-v_{S-}^2/2q$, or in normalized form

$$\varphi(\xi_r)=\beta_+ +\beta_- \ . \tag{5.6}$$

This value of the potential is independent on the negative-ion density. Equation (5.6) is valid exactly for $\Theta=\infty$ and can be used as an approximation also for $\Theta \gg 1$ for the value of the electric potential at the reflection point, where the field intensity is minimal $\varphi(E_{\min})=\varphi(\xi_r)$. The potential at the point where the electric field is maximum depends on α. For $\alpha=\alpha^*$ and $\Theta=\infty$ a linear dependence in β_+ and β_- can be obtained from the numerical results

$$\varphi(E_{\max})=0.048+0.97\beta_+ +0.8\beta_- \tag{5.7}$$

or equivalently

$$U(E_{\max})\approx U_S-\frac{0.4m_-}{q}v_{S-}^2 \ . \tag{5.7a}$$

The dependence (5.7) of $\varphi(E_{\max})$ on β_+ for different β_- is shown in Fig. 9. $E_{\max}(\beta_+,\beta_-)$ is plotted in Fig. 10. It is seen that for $\Theta=\infty$ the maximum electric field is determined mainly by the kinetic energy of the negative ions streaming into the sheath. For $\Theta=\infty$ a series approximation in $\zeta=E_{\max}/E^*$ can be derived:

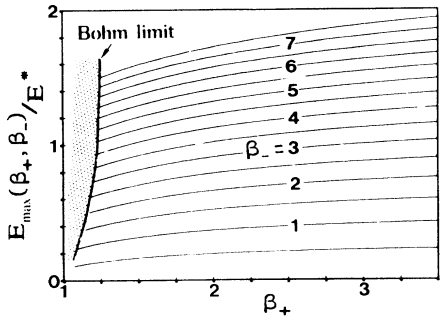

FIG. 10. Dependence of $E_{\max}$ on β_+ and β_- for $\alpha=\alpha^*$ and $\Theta=\infty$.

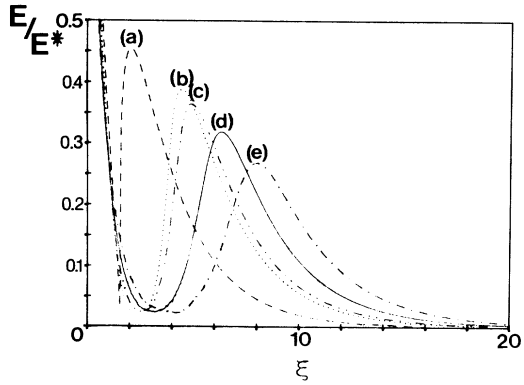

FIG. 11. $E(\xi)$ at $\alpha \approx \alpha^*$ for various ion temperatures: (a) $\Theta=\infty$, $\alpha=0.1065$, (b) $\Theta=1000$, $\alpha=0.1242$, (c) $\Theta=500$, $\alpha=0.1307$, (d) $\Theta=200$, $\alpha=0.1409$, and (e) $\Theta=100$, $\alpha=0.1506$.

$$\beta_- = 3.44\zeta(1-0.1308\beta_+)(1+0.30465\zeta+0.0487\zeta^2 +0.0102\zeta^3) . \quad (5.8)$$

Relations (5.7) and (5.8) are valid in the limit $T_i/T_e \to 0$. The dependence of $E_{\max}$ on Θ can be seen in Fig. 11, where the $E(\xi)$ dependences are shown for different Θ values for $\alpha \approx \alpha^*$.

VI. INFLUENCE OF THE EMISSION OF SECONDARY ELECTRONS

The emission of secondary electrons at the electrode is an important process in the mechanism of glow discharges. It also influences the structure of the boundary sheath. The model used here is easily extended to these electrons. The emission of the secondary electrons by the impact of positive ions on the electrode is modeled in this section by an additional electron flow with the density $n_{S\gamma}=\gamma n_S$ and the average velocity $v_{S\gamma}$ at $x=x_S$ with a thermal velocity spread characterized by the temperature $T_\gamma=\vartheta T_e$. At $x=x_S$ the plasma is considered to be quasineutral, so that $n_S=n_{S+}=n_{Se}+n_{S\gamma}+n_{S-}$.

A. The structure of the field in the sheath

The motion of the secondary electrons again is considered collisionless in the boundary sheath, so that the density n_γ of the secondary electrons inside the sheath can be obtained from the energy conservation and continuity equation as a function of the electric potential. Introducing this additional density in the Poisson equation (3.13), the influence of the secondary electrons on the field in the sheath can be determined. After integration, an equation similar to Eq. (3.15) results with the function $f(\varphi)$ given by

$$f(\varphi)=(1-\gamma)\left[\frac{1}{1+\alpha}\left[\exp\left[\frac{\beta_+-\varphi}{2}\right]-1\right]\right.$$
$$+\frac{\alpha\beta_+\kappa}{1+\alpha}\left[\frac{\Theta\beta_+\kappa}{2\pi}\right]^{1/2}\int_{\eta^*}^{\infty}\left\{\left[(\eta+1)^2+\frac{1}{\kappa}\left[1-\frac{\varphi}{\beta_+}\right]\right]^{1/2}-\eta-1\right\}(\eta+1)\exp\left[-\frac{\Theta\kappa\beta_+}{2}\eta^2\right]d\eta$$
$$+\gamma\mu\beta_+\left[\frac{\vartheta\beta_+\mu}{2\pi}\right]^{1/2}\int_{\eta_\gamma}^{\infty}\left\{\left[(\eta+1)^2+\frac{1}{\mu}\left[1-\frac{\varphi}{\beta_+}\right]\right]^{1/2}-\eta-1\right\}(\eta+1)\exp\left[-\frac{\vartheta\mu\beta_+}{2}\eta^2\right]d\eta$$
$$\left.+\beta_+\left[\frac{\Theta\beta_+}{2\pi}\right]^{1/2}\int_{-1}^{\infty}\left[\left[(\eta+1)^2-1+\frac{\varphi}{\beta_+}\right]^{1/2}-\eta-1\right](\eta+1)\exp\left[-\frac{\Theta\beta_+}{2}\eta^2\right]d\eta\right] . \quad (6.1)$$

Here the notations

$$\eta_\gamma=-1+\left[\frac{1}{\mu}\left[\frac{\varphi_0}{\beta_+}-1\right]\right]^{1/2},$$

$$\varphi_0=\frac{m_+v_{S+}^2-2q(U_0-U_S)}{kT_e},$$

$$\mu=\frac{m_ev_{S\gamma}^2}{m_+v_{S+}^2}=\frac{\varphi_0}{\beta_+}-1+\varepsilon,$$

and

$$\varepsilon=\frac{m_ev_{0\gamma}^2}{m_+v_{S+}^2},$$

are introduced with the potential U_0 at the electrode and the emission velocity $v_{0\gamma}$ of the secondary electrons. Typical results for plasmas with negative ions and without negative ions are shown in Figs. 12 and 13. The secondary electrons change the electric field to lower values especially in the vicinity of the electrode, where they are moving slowly, and in the region where the negative ions are reflected. The influence of the secondary

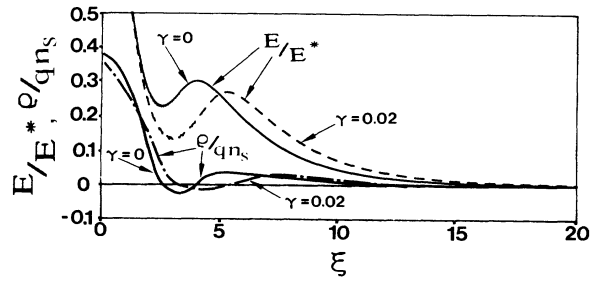

FIG. 12. The influence of the secondary electrons ($\gamma=0$ and 0.02) on the structure of the electric field and of the charge density in the sheath for plasmas with negative ions for $\Theta=100$, $\beta_+=1.5$, $\alpha=0.138$, $\kappa=1$, $\vartheta=10$, and $\varepsilon=1$.

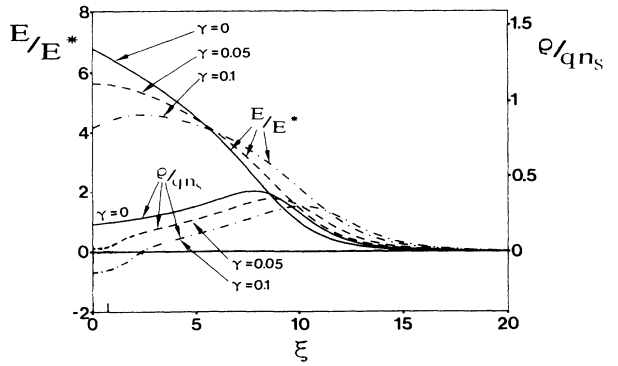

FIG. 13. The influence of the secondary electrons ($\gamma=0$, 0.05, and 0.1) on the structure of the electric field and of the charge density in the sheath for plasmas without negative ions for $\Theta=100$, $\beta_+=1.5$, $\alpha=0$, $\kappa=1$, $\vartheta=10$, and $\varepsilon=1$.

electrons increases if the relative density γ of these electrons increases and if their initial velocity $v_{0\gamma}$ decreases. The thermal velocity spread is of negligible influence for $5<\vartheta<100$. For large values of γ and small values of $v_{0\gamma}$ the electron density in the vicinity of the electrode becomes larger than the positive-ion density and a "virtual cathode" develops. In this case the electric field has an additional maximum in the sheath.

B. Bohm's criterion in the presence of secondary electrons

Similar to Sec. IV 4, Bohm's criterion can be derived from Eq. (6.1):

$$\frac{1-\gamma}{1+\alpha}-\frac{(1-\gamma)\alpha}{(1+\alpha)\beta_-}-\frac{\gamma}{\beta_\gamma}-\frac{1}{\beta_+}>0 \tag{6.2}$$

with $\beta_\gamma=m_e v_{S\gamma}^2/kT_e$. Therefore the secondary electrons lead to an increase of the limit for v_{S+} compared to the case $\gamma=0$.

For a plasma with no negative ions there results from (6.2)

$$\frac{\gamma}{\beta_\gamma}+\frac{1}{\beta_+}<1-\gamma\ . \tag{6.3}$$

This relation can be interpreted similar to Eq. (4.4) in Fig. 3.

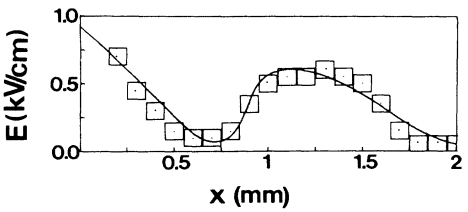

FIG. 14. Experimental points of Ref. [10] (small squares) and the theoretical curve for the electric field (solid line) with $\alpha=0.727$, $\beta_+=45$, $\kappa=0.95$, $\Theta=100$, $T_e=2.1$ eV, and $n_e=1.16\times10^{10}\,\mathrm{cm}^{-3}$.

VII. COMPARISON WITH EXPERIMENTS

Measurements of the electric field in the cathode fall are published in the papers of Gottscho *et al.* [9,10] for rf glow discharges at 50 kHz in BCl_3. In both cases double layers are observed in the cathode sheath [see Fig. 8 of Ref. [9] for $\pi<\omega t\le\frac{13}{10}\pi$ and Fig. 3(b) of Ref. [10] for $\omega t=\frac{11}{10}\pi$]. These figures are similar to Figs. 6, 8, 11, and 12 of this work.

For a comparison of the experimental results with theory, Fig. 3(b) of Ref. [10] for $\omega t=\frac{11}{10}\pi$ is reproduced here in Fig. 14 by the small squares. One of the theoretical curves obtained by integration of Eq. (3.15) is given by the solid line. Good agreement between the theoretical and experimental results is obtained with the parameter values indicated in Fig. 14.

The integral (3.15) with $f(\varphi)$ given by (6.1) depends on the eight parameters α, β_+, γ, ε, μ, ϑ, κ, and Θ. Therefore many possibilities to get good agreement with the experimental values of Fig. 14 exist also for other parameter combinations. Such examples are given in Table I. Here it is assumed that $\Theta=100$ and that the coupling between the positive and negative ions in the bulk plasma and in the presheath by Coulomb collisions is strong enough to take $\kappa=0.95$. For β_+ different values in the interval $20\le\beta_+\le52$ were chosen. For each β_+ value the parameter α was varied until the best agreement of the theoretical curve with the experimental values was obtained. The Debye length λ_D and the electric field E^* are determined by comparison of the theoretical curves with the experimental results. From λ_D and E^* the electron temperature T_e and the electron density n_e are calculated for each case. From the computed values given in Table I the product β_+kT_e is constant. This is a result of the

TABLE I. Several parameter sets that describe the experimental values shown in Fig. 14 as described in the text.

α	β_+	γ	κ	ε	λ_D (mm)	$-E^*$ (kV/cm)	kT_e (eV)	n_e (cm^{-3})	β_+kT_e (eV)
0.695	20	0	0.95		0.15	0.155	4.65	1.14×10^{10}	93
0.702	25	0	0.95		0.135	0.14	3.78	1.14×10^{10}	94.5
0.708	30	0	0.95		0.125	0.13	3.25	1.15×10^{10}	97.5
0.715	35	0	0.95		0.115	0.12	2.76	1.15×10^{10}	96.6
0.721	40	0	0.95		0.107	0.11	2.35	1.13×10^{10}	94.2
0.727	45	0	0.95		0.1	0.105	2.1	1.16×10^{10}	94.5
0.67	52	0.1	0.95	0.025	0.087	0.104	1.81	1.32×10^{10}	94.1

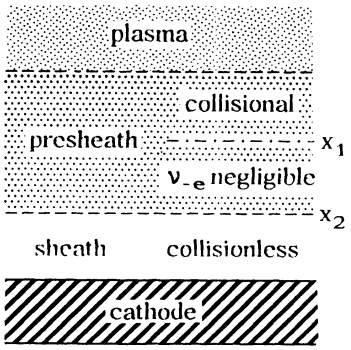

FIG. 15. The change of the collision process in the vicinity of the cathode.

energy conservation: the kinetic energy of the negative ions at $x=2.25$ mm must be equal to the potential energy at the reflection point at $x\approx 0.75$ mm. The potential energy can be obtained by integrating the experimental field intensities from $x=2.25$ mm to $x\approx 0.75$ mm, with the result $\frac{1}{2}m_- v_{S-}^2 \approx 45$ eV. This leads to $\beta_+ kT_e = m_- v_{S-}^2/\kappa \approx 94.7$ eV. The calculated numerical values of T_e and n_e in Table I are reasonable. The large value of β_+ is surprising, and is a result of the following effect: Because of the large difference in the presheath between the collision frequencies ν_{-+} and ν_{-e} [see Eqs. (2.4)–(2.6)], there exists a distance x_1 from the cathode (Fig. 15), where the collisions of the ions with the electrons can be neglected. The collisions between the negative ions and positive ions are still important and the negative ions are still captured by the positive-ion beam at x_1 until they reach the distance x_2 near the cathode, where ν_{-+} is also negligible. The basic equations (3.6)–(3.14) are valid within the collisionless sheath between the interface x_2 and the cathode. In the interval between x_1 and x_2 a separation of the electron gas from the ion beam begins and the plasma is non-neutral in the region $x_1 > x > x_2$. Here strong electric forces accelerate the positive ions and with them the captured negative ions before they reach x_2. This effect explains the large β_+ values.

VIII. CONCLUSIONS

The structure of the plasma boundary sheath (electric field, particle motion, charge distribution, Bohm criterion) determines the physical processes at the electrode surface, the current-voltage characteristics and the floating potential. For applications of plasmas to materials processing, e.g., thin-film etching and deposition, the processes in the boundary layer between the plasma and the surface is of paramount importance. In the present paper the traditional theory of the collisionless sheath for plasmas with positive ions is extended to plasmas containing also negative ions and secondary electrons. It is shown that for small concentration of the negative ions, these ions can be captured by the positive-ion flow and can be reflected inside the sheath. This process can explain the experimentally observed double layers [9,10] and the corresponding maximum of the electric field in the sheath. A second process, which can lead to a maximum of the electric field in the collisionless boundary sheath is the emission of the secondary electrons at the electrode. In this case a "virtual cathode" can develop.

ACKNOWLEDGMENT

The authors thank Professor R. Wienecke for his interest in this work.

[1] L. Tonks and I. Langmuir, Phys. Rev. **34**, 876 (1929).
[2] D. Bohm, *The Characteristics of Electric Discharges in Magnetic Fields* (McGraw-Hill, New York, 1949), p. 77.
[3] F. F. Chen, *Plasma Physics and Controlled Fusion* (Plenum, New York, 1984), p. 292.
[4] R. Deutsch and E. Räuchle, Plasma Chem. Plasma Proc. **11**, 501 (1991).
[5] N. St. J. Braithwaite and J. E. Allen, J. Phys. D **21**, 1733 (1988).
[6] H. Amemiya, J. Phys. D **23**, 999 (1990).
[7] H. Shindo and Y. Horiike, Jpn. J. Appl. Phys. **30**, 161 (1991).
[8] K.-U. Riemann, J. Phys. D **24**, 493 (1991).
[9] R. A. Gottscho, C. E. Gaebe, IEEE Trans. Plasma Sci. **PS-14**, 92 (1986).
[10] R. A. Gottscho, Phys. Rev. A **36**, 2233 (1987).
[11] R. A. Gottscho, A. Mitchell, G. R. Scheller, Y.-Y. Chan, and D. B. Graves, Phys. Rev. A **40**, 6407 (1989).
[12] J. P. Boeuf, Phys. Rev. A **36**, 2782 (1987).
[13] F. A. Haas, L. M. Lea, and A. J. T. Holmes, J. Phys. D **24**, 1541 (1991).
[14] D. L. Book, *NRL Plasma Formulary* (Naval Research Laboratory, Washington, DC, 1978), p. 26.

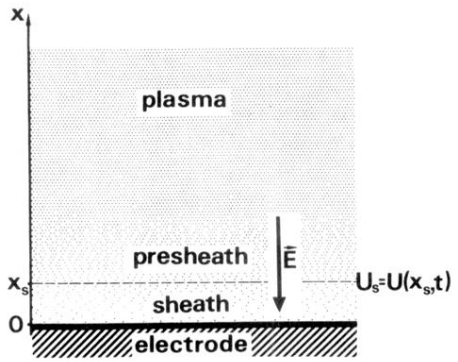

FIG. 1. Geometry of the plasma and plane electrode and notation.

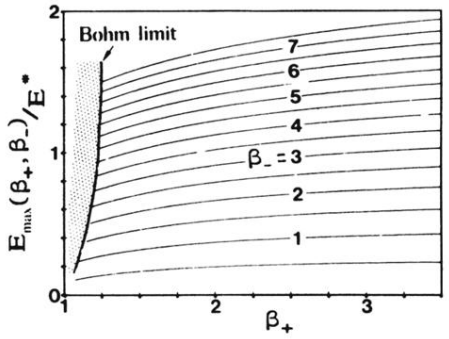

FIG. 10. Dependence of $E_{\max}$ on β_+ and β_- for $\alpha=\alpha^*$ and $\Theta=\infty$.

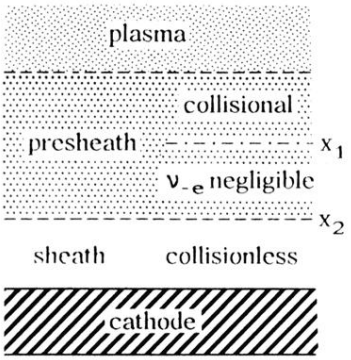

FIG. 15. The change of the collision process in the vicinity of the cathode.

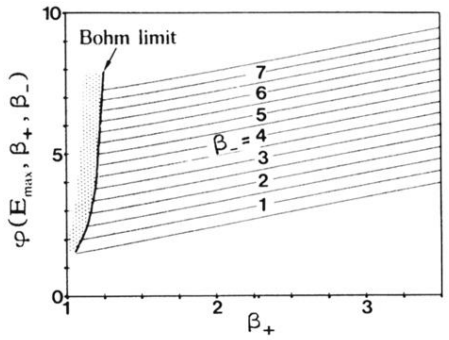

FIG. 9. $\varphi(E_{\max})$ as a function of β_+ and β_- for $\alpha=\alpha^*$ and $\Theta=\infty$.